PROGRESS TOWARDS SUSTAINMENT OF ADVANCED TOKAMAK MODES IN DIII–D*

B.W. RICE,† K.H. BURRELL, J.R. FERRON, C.M. GREENFIELD, G.L. JACKSON, L.L. LAO, R.J. LA HAYE, T.C. LUCE, B.W. STALLARD,† E.J. STRAIT, E.J. SYNAKOWSKI,‡ T.S. TAYLOR, A.D. TURNBULL, M.R. WADE◊
DIII–D National Fusion Facility, General Atomics, San Diego, California, U.S.A.

Abstract

Improving confinement and beta limits simultaneously in long-pulse ELMy H–mode discharges is investigated. The product $\beta_N H_{98y}$ serves as a useful figure-of-merit for performance, where $\beta_N \equiv \beta/(I/aB)$ and H_{98y} is the ratio of the thermal confinement time relative to the most recent ELMy H–mode confinement scaling established by the ITER confinement database working group. In discharges with $q_{min} > 1.5$ and negative central magnetic shear, $\beta_N H_{98y} \sim 4$ is sustained for ~1 s. Although peaked profiles are observed, strong internal transport barriers are not present. Further increases in β_N in these discharges is limited by neoclassical tearing modes (NTM) in the positive shear region. In another recently developed regime, $\beta_N H_{98y} > 6$ has been sustained during large infrequent ELMs in non-sawtoothing discharges with $q_0 \sim 1$. This level of performance is similar to that obtained in ELM-free regimes such as VH–mode. The limitation on β_N and pulse length in these discharges is also the onset of NTMs.

1. INTRODUCTION

Advanced Tokamak (AT) operating modes have been successful in improving the fusion performance of many existing tokamaks, as evidenced by the record D-D fusion reactivity achieved in DIII–D [1], JET [2], and JT-60U [3]. Through optimization of the plasma shape and radial profiles, AT modes lead to improved confinement and β, and higher bootstrap fraction relative to standard ELMy H–mode. Improvements are observed in many different AT regimes such as VH–mode, negative central shear (NCS) with an internal transport barrier (ITB), supershots, high β_p, and high ℓ_i. To date, however, the duration of peak performance in all of these modes is limited to a few energy confinement times (τ_E), generally as a consequence of evolving pressure or current profiles and eventual MHD instability. Before AT modes can be seriously considered as an operating mode for a future fusion reactor, present experiments must sustain AT performance in a controlled manner for longer pulse lengths. In this paper, we review results of recent experiments on DIII–D directed towards this goal

The primary focus is on improving the performance and pulse length of discharges with an ELMy edge. The ELMy H–mode is inherently steady state, with the edge p' and impurity concentration regulated by the repetitive ELM events. The ELMy H–mode regime has been studied extensively on most tokamaks and the confinement results have been compiled into a database by the ITER confinement database working group. The most recent scaling for the thermal energy confinement time is given by $\tau_{th}^{98y} = 0.0365 I_p^{0.97} R^{1.93} (a/R)^{0.23} n_{19}^{0.41} B^{0.08} M^{0.2} \kappa^{0.67} P^{-0.63}$ [4]. This scaling was generated from mostly sawtoothing ELMy H–modes with monotonic q profiles and $q_0 \sim 1$.

The most serious limitation on β in long-pulse ITER-like discharges appears to be the neoclassical tearing modes (NTM) [5,6]. NTM modes are classically stable tearing modes ($\Delta' < 0$) that are driven unstable by a helically perturbed bootstrap current. The NTM mode requires a seed island to exceed a minimum threshold island width; this seed island can be provided by a sawtooth crash or other MHD perturbation. Depending on the density (or collisionality ν^*), NTMs limit β_N to the range $\beta_N \sim 1.7–2.5$.

*Work supported by U.S. Department of Energy under Contracts DE-AC03-89ER51114, DE-AC05-96OR22464, and Grant No. DE-FG03-95ER54294.
†Lawrence Livermore National Laboratory, Livermore, California, U.S.A.
‡Princeton Plasma Physics Laboratory, Princeton, New Jersey, U.S.A.
◊Oak Ridge National Laboratory, Oak Ridge, Tennessee, U.S.A.

Our goal is to sustain higher β and confinement time relative to the ITER benchmark to achieve a more compact reactor concept with a high bootstrap fraction. The normalized quantity $\beta_N H_{98y}$ serves as a useful figure-of-merit for performance, where $H_{98y} \equiv \tau_{th}/\tau_{th}^{98y}$. At the 1996 IAEA conference, DIII–D reported on non-sawtoothing discharges (#89756, #89795) with H_{98y}~1.4 (H_{89p}~2.4) and β_N~2.9 sustained for up to 2 s in lower single null with triangularity of δ=0.3 [7]. These discharges utilized 1.2 MW of beam power during the I_p ramp to suppress sawteeth and cryopumping to maintain low density. Fishbone (m/n=1/1) bursts were observed throughout the high performance phase and appear to play a role in regulating the on-axis current to maintain q_0~1 thus avoiding sawteeth. Due to the absence of a sawtooth triggered seed island, the value of β_N achieved was almost a factor of 2 above the predicted NTM limit at the operational density (collisionality) However, fishbones can also provide a seed island for the NTM, limiting both the reproducibility of this regime and attempts to further increase β_N.

Here we present recent results from two campaigns designed to improve these earlier results. First, techniques to produce and sustain q_{min}>1.5 in ELMy H–mode are explored. The motivation for this work is to eliminate fishbones and eliminate the 3/2 surface (and possibly the 2/1 surface) so that the NTM β_N limit can be increased. This work is also motivated by the possibility of obtaining a sustained internal transport barrier (ITB) to further improve the confinement of ELMy H–modes. Second, we report on discharges obtained with a new shape and startup technique that yielded very high confinement (H_{98y} ~2) and beta (β_N~4) during infrequent ELMs with monotonic q profiles. These discharges reached performance levels comparable to ELM-free modes such as VH–mode and sustained this level up to 1 s.

2. ELMy DISCHARGES WITH q_{min}>1.5

Current profiles with negative central shear and q_{min}>1.5 are routinely obtained by heating with P_{NBI}~5 MW during the current ramp with an L–mode edge. However, the development of ITBs in these plasmas results in pressure peaking that is difficult to control and often leads to disruption. Also, because of the cold L–mode edge, the current profile and q_{min} evolve more quickly making sustainment difficult. To avoid these problems, a new startup technique has been developed using H–mode during the current ramp as shown in Fig. 1(a). A brief flat spot in the current ramp at 400 ms, coupled with the biasing of the plasma shape toward lower null point in the ion ∇B drift direction, leads to a reproducible H–mode transition. By controlling the I_p ramp rate and the density, values of ℓ_i

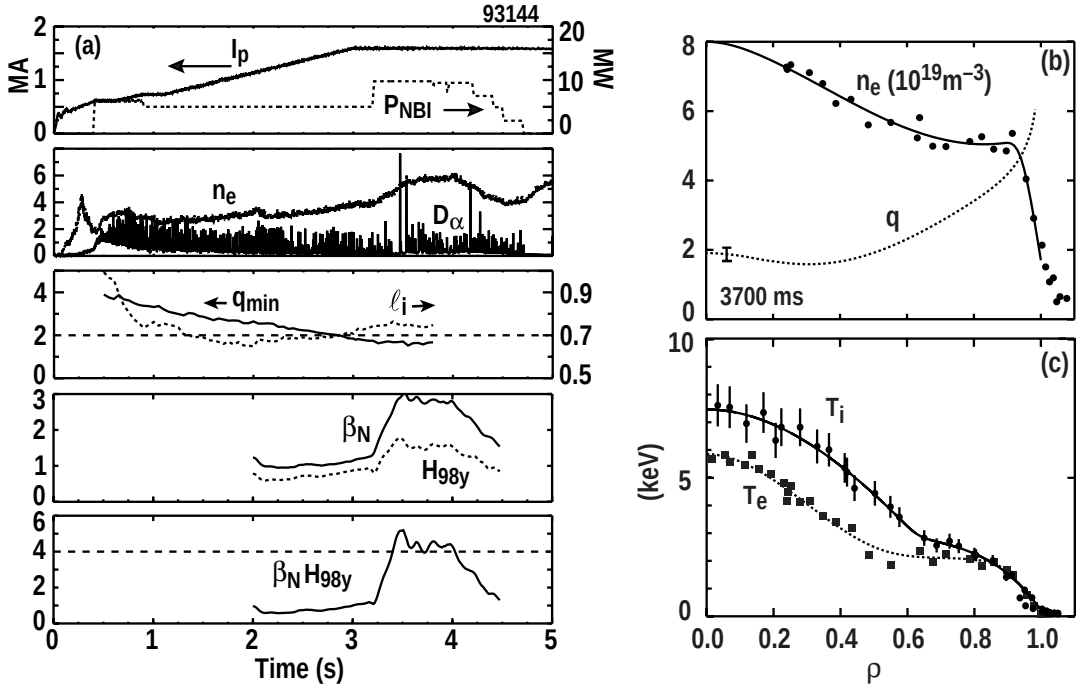

Fig. 1. (a) Time evolution of q_{min}>1.5 discharge (93144) with high performance from 3.5–4 s. (b) Profiles of n_e and q and (c) T_e and T_i at 3.7 s. (B_T=2.1 T, high triangularity shape with δ=0.77, κ=1.85; H_{89p}=2.5 at 3.7 s)

as low as 0.5 can be obtained, although for ℓ_i <0.6 edge stability problems can lead to locked-modes during the I_p ramp. The best results are obtained with a slower I_p ramp and ℓ_i ~ 0.7 as shown in Fig. 1(a).

The high performance phase extends from 3.4–4 s where $\beta_N H_{98y}$~4.2 is sustained for 0.5 s. The high power phase is relatively short in this discharge due to the long formation phase and the termination of P_{NBI}. Similar discharges sustained somewhat reduced $\beta_N H_{98y}$~3.8 for 1.5 s, but these all suffered from continuous NTM activity. Discharge 93144 in Fig. 1 is free from any significant MHD mode. The profiles of q, n_e, T_e, and T_i at 3.7 s are shown in Fig. 1(b) and 1(c). The density profile is more peaked than standard ELMy H–mode, but comparable to the other improved performance discharges such as those discussed in the introduction with a monotonic q profile. The T_i and T_e profiles show a somewhat steeper gradient at ρ~0.5 than is observed in monotonic q profile discharges, indicating a weak ITB. However, the ITB is much weaker here than in low density L–mode edge NCS discharges at comparable power. We note that the line average density in H–mode is ~2 times that in L–mode edge NCS discharges, and with this density level we would not expect to observe strong ITBs with an L–mode edge either. The shear reversal [Fig. 1(b)] is weaker in these ELMy H–mode discharges compared with L–mode edge NCS discharges with an ITB. It could be argued that the ITB only forms with strong NCS, but there is evidence on DIII–D that ITBs can form at low density even with monotonic q profiles [8]. Rather, it appears that strong ITBs reinforce the hollow current profile through the off-axis bootstrap current, thus leading to stronger shear reversal.

Although sawteeth and fishbones are not present in the NCS discharges, NTMs continue to be the limiting instability as illustrated by the growth of a resistive m/n=5/2 mode in discharge 93149 shown in Fig. 2. This discharge is similar to 93144 in Fig. 1 except that P_{NBI} is increased to ~ 12 MW. For NTM modes, we expect the mode amplitude to scale with β_N^2, which roughly holds as shown in Fig. 2(b). The classical tearing stability parameter Δ' was calculated to be negative for this discharge indicating that it should be stable to the classical mode. Although the NTM is not catastrophic in this case, it does result in a saturation of β_N. Despite the increased P_{NBI}, β_N is actually slightly less in 93149 compared with 93144 which has no MHD mode. Note that the mode already exists at a low level in Fig. 2 prior to the step up in P_{NBI} at 2.8 s. For this series of discharges the fast magnetics data on DIII–D was set to cover the high power phase only (t >2.35 s), so it is not clear what initiates the low level mode present at 2.4s. One speculation is that the mode begins as q_{min} passes through q=5/2 at ~ 2 s, then grows later when P_{NBI} is increased.

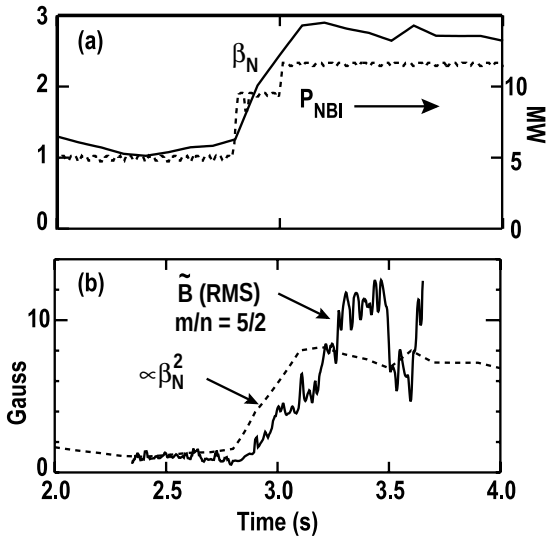

FIG. 2. (a) Time evolution of β_N and P_{NBI} for a q_{min}~2 discharge with NTM activity. (b) Fluctuation amplitude scales with β_N^2 as expected for NTMs.

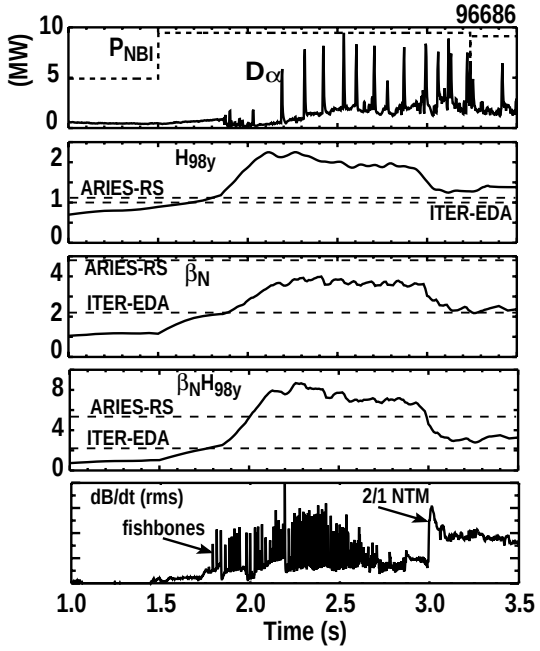

FIG. 3. Time evolution of discharge 96686 with β_N ~3.8 and H_{98y}~2 (H_{89p}~3.2) sustained for 1 s during infrequent ELMs. Dashed lines indicate the ITER-EDA design and ARIES-RS reactor study requirements for β_N and H_{98y}.

3. HIGH–PERFORMANCE REGIME WITH INFREQUENT ELMS

A new regime has been developed in DIII–D where performance equivalent to ELM-free modes such as VH–mode is sustained through many low frequency ELMs. As shown in Fig. 3, β_N~3.8, H_{98y}~2, and $\beta_N H_{98y}$>6 are sustained for 1 s. Lines indicating the β_N and H_{98y} values required for ITER-EDA and the ARIES-RS reactor study are also shown, indicating that this discharge exceeds the ARIES-RS requirements for the $\beta_N H_{98y}$ product. The q profile is monotonic with q_0~1 and 1/1 fishbones (but no sawteeth) are present throughout the high performance phase. Some parameters of interest during the high performance phase are: β_t~4.5%, n_e/n_{Gr}~0.5, q_{95}=4.4, τ_{th}~0.21 s and f_{bs}~50%, where n_{Gr} is the Greenwald density and f_{bs} is the bootstrap fraction. The high performance phase is terminated at ~3 s by the initiation of a m/n=2/1 NTM. Although difficult to judge from Fig. 3, when the NTM begins, the ELM frequency increases to a level more typical of ELMing H–modes at these operational parameters.

Determining the key elements for accessing this regime is still under investigation, but several operational characteristics can be identified. The initiation of a discharge similar to that shown in Fig. 3 is shown in Fig. 4. This discharge reaches slightly higher values of β_N and H_{98y} compared with Fig. 3, but the duration is shorter ~0.7 s. The discharge begins with a fast I_p ramp of ~10 MA/s to 1 MA, followed by a slow ramp rate to the final current of 1.6 MA. Beam power of 5 MW is injected at 0.1 s, leading to an extremely hollow J profile (ℓ_i ~0.3) with ρ_{qmin}~1 at 0.2 s. MHD modes due to the unstable skin current profile cause the current to penetrate rapidly leading to a weak NCS profile at 0.5 s. By the time the beams step up to full power (all co-current beam injection), the q profile has evolved to be monotonic with q_0~1, ℓ_i~1.1, and fishbones are present.

An important feature of these discharges is the plasma shape (see bottom of Fig. 4). A high triangularity (δ=0.77, κ=1.85) single null shape with the X-point at the top of the vessel is utilized. The ion ∇B drift direction is down which raises the H–mode transition power threshold significantly. With this shape it takes 0.5 s at P_{NBI}=9.5 MW before the H–mode transition occurs. This long L–mode phase allows an ITB to form prior to the H–mode transition (H_{98y} ~ 1 in L–mode at 2 s) which enhances the performance after the H–mode transition is made. This technique has been used previously to maximize the fusion power in DIII–D [1], but in those cases the double null shape was symmetrized after the H–mode transition and high performance extended through the ELM-free phase only. In these discharges, the shape remains single null with the X–point at the top and close to the wall throughout the discharge.

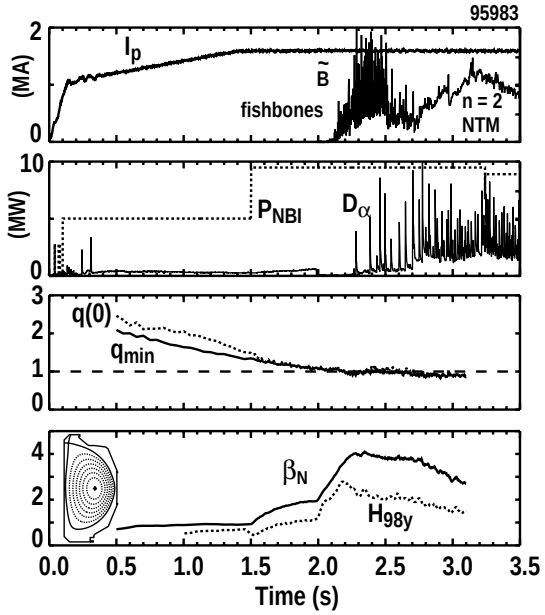

FIG. 4. Time evolution of 95983, illustrating the formation phase and q profile evolution. β_N~3.9 is sustained during infrequent ELMs from 2.2–2.7 s.

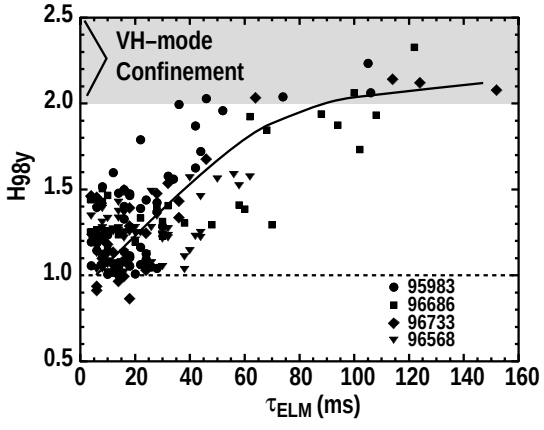

FIG. 5. Confinement enhancement, H_{98y}, improves with period between ELMs. Shaded region indicates typical confinement range for VH–modes on DIII–D.

The exact importance of the startup and plasma shape is not clear. Since the target q profile is simply monotonic with q_0~1, we believe that the early fast I_p ramp and early beam power should not be critical. However, we have been unable to reproduce this regime without a startup similar to that used in Fig. 4. The shape probably plays a more important role, since edge stability is sensitively dependent on edge parameters such as p', J_{95} and collisionality. Also, the close proximity of the X–point to the wall results in higher than usual recycling.

The infrequent ELMs also appear to play a significant role in achieving sustained high confinement. In Fig. 5, the time between ELMs (τ_{ELM}) is plotted versus the H_{98y} at the time of the ELM for several discharges. For τ_{ELM}<20 ms, confinement is close to standard ELMy H–modes with H_{98y}~1 (this represents the later part of these discharges after beta collapses). As τ_{ELM} increases to ~100 ms, confinement similar to VH–mode [9] levels is obtained. The energy loss per ELM can be quite large in this regime, ranging from 2%–5% of the plasma stored energy. With the long period between ELMs, however, the stored energy quickly recovers after the ELM. Infrequent ELMs are necessary but not sufficient to achieve the higher performance. For example, low power ELMy discharges often have infrequent ELMs but the confinement is not significantly improved.

Another factor in these discharges is that the toroidal rotation and the resulting radial electric field and E×B shear are sustained through the infrequent ELMs. For discharge 95983 in Fig. 4, $v_\phi(0)$~320 km/s and $E_r(\rho\sim0.5)$ ~120 kV/m are sustained from 2.2–2.7 s.

Profiles for discharge 95983 (Fig. 4) at 2250 ms, just before the first ELM, are shown in Figs. 6(a–e). For comparison, the profiles of a VH–mode with the same beam power and plasma current are also plotted for a time slice just before the first ELM. In the case of the VH–mode, plasma performance returns to standard ELMing H–mode after the 1st ELM. One clear difference between the two regimes is the peaking of density in 95983 compared with the VH–mode which shows a hollow density profile typical of VH–modes. The high edge density in VH–mode is correlated with the high edge Z_{eff} seen in Fig. 6(b). Compared with the VH–mode, discharge 95983 has somewhat higher Z_{eff} in the core (due to startup conditions) but a lower Z_{eff} at the edge. After the first few ELMs the edge Z_{eff} in 95983 is reduced to < 3.

Transport analysis has been performed using the TRANSP code for discharge 95983. In Fig. 6(f), the experimental diffusivities χ_i and χ_e are plotted along with the neoclassical calculation for χ_i during the ELMing phase. For this figure, the χ's are averaged over 200 ms during the ELMing phase to smooth over the ELM fluctuations. The reduction in χ_i relative to a standard ELMing H–mode is about 2–3, while χ_e is reduced a more modest amount. Note that there is no indication of an abrupt internal transport barrier, χ_i is simply reduced uniformly across the plasma. Although not plotted here, during the ELM-free phase of 95983, χ_i is equal to the neoclassical χ_i (within error bars) over most of the plasma radius as seen in other high performance discharges [1].

3.1. Edge Stability Analysis

The discharges shown in Figs. 3 and 4 do not collapse at the first ELM as do VH–modes [10], for example. Early speculation on why these ELMs are more benign focused on the possibility that the

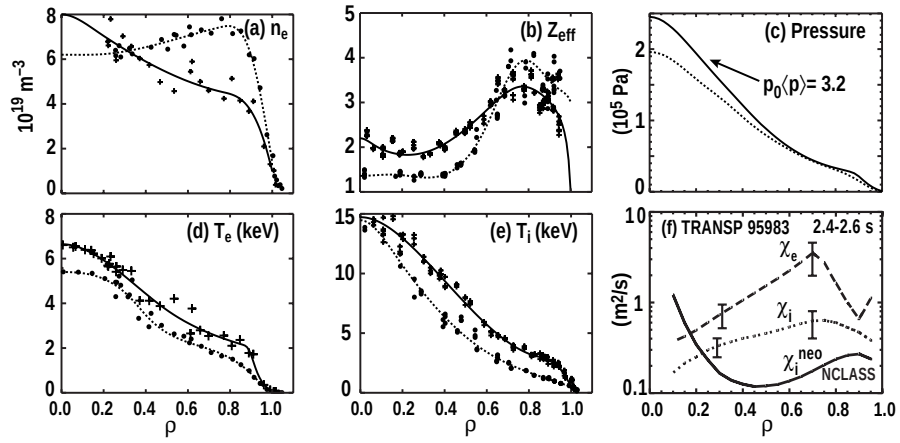

FIG. 6. (a–e) Profiles for 95983 at 2.25 s, just before the first ELM (solid curves and plus symbols) and VH–mode profiles (83710 at 2.75 s) just before the first ELM (dashed curves and sold circles). (f) χ profiles for 95983 during ELMs (2.4-2.6 s) calculated from TRANSP.

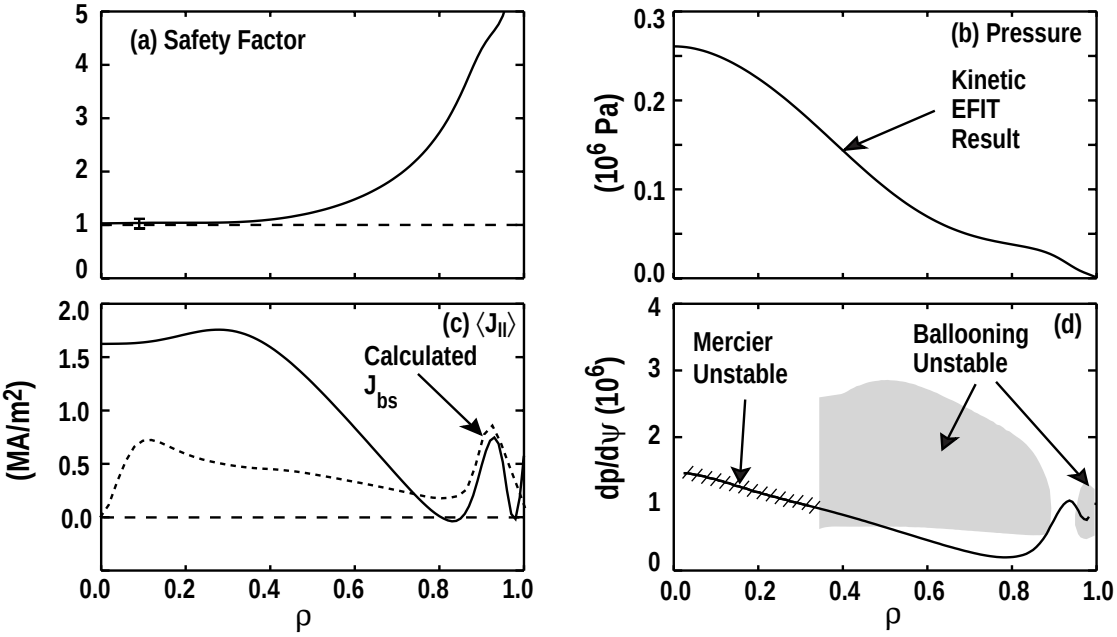

FIG. 7. (a–-c) Kinetic EFIT equilibrium profiles for 95983 at 2.25 s. The dashed line in (c) represents the calculated bootstrap current density for the profiles shown in Fig. 6. (d) Ballooning/Mercier stability diagram at 2.25 s. The solid curve is the experimental value of dp/dψ.

edge p′ was reduced. However, as seen in Fig. 6, although the density gradient is substantially reduced compared with VH–mode, the temperatures are higher, so that the final edge pressure gradient and pedestal height are actually higher in 95983 than the VH–mode. Profiles of q, p, and $\langle J_{||} \rangle$ from a kinetic efit prior to the first ELM at 2.25 s are shown in Fig. 7. The EFIT equilibrium reconstruction utilizes external magnetic measurements, MSE data–including E_r corrections–and pressure profiles including the calculated fast ion contribution. The q profile shows a large flat region with q~1 while the current density shows a large edge current peak due to the edge p′ and the resulting bootstrap current. Calculations of the bootstrap current density is shown in Fig. 7(c). The location and amplitude of the measured bootstrap peak is in good agreement with this calculation. Note that the overall current at the edge is somewhat reduced because the edge surface voltage is actually negative during the ELM-free phase leading up to this time. Ballooning and Mercier stability have been calculated with the results plotted in Fig. 7(d). The reduction in edge shear due to the edge bootstrap current opens up 2nd stability access at ρ~0.95 which allows the high edge pressure gradient. This result is typical of most ELM-free, high triangularity plasmas on DIII–D. The core is Mercier unstable due to low value of q inside ρ~0.35 and the large pressure gradient in this region. We note that recent theoretical work on the stabilizing effects of fast ions may modify the Mercier criterion in this region [11].

GATO calculations of ideal n=1–4 stability has also been performed for this timeslice. In general, GATO predicts that this regime is marginally stable to n≥1 edge "peeling" modes, although depending on the exact details of how the input equilbria is prepared, GATO can also find these modes to be unstable. The important point, however, is that experimentally there seems to be no coupling between the edge mode and a more destructive global mode. The reasons for this are not known, but we suspect that unique features of the shape and edge current profile may be playing a role. Despite the large current spike observed at ρ~0.95 in Fig. 7(c), the average current from $0.75 < \rho < 1$ is not so high at this time because the surface loop voltage is slightly negative.

3.2. NEOCLASSICAL TEARING MODES

All of the discharges produced to date that achieve high performance (β_N>3.5) during ELMs revert to a standard H–mode with a soft beta collapse accompanied by MHD activity that has the characteristic signature of the NTM. These characteristics are that (1) $\Delta' < 0$ indicating modes are classically stable; (2) a seed island threshold width must be exceeded before the mode can grow; (3) the mode amplitude saturates at a level that can be predicted by NTM theory and is $\propto \beta_N^2$. Since none of these discharges have sawteeth, the seed island must be generated by another mechanism. In

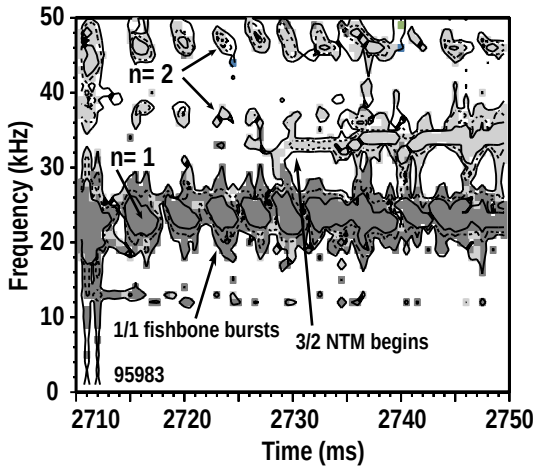

FIG. 8. Contours of constant B-dot mode amplitude for n=1 (dark shade) and n=2 (light shade) modes. A continuous 3/2 mode is triggered by a fishbone burst at 2730 ms.

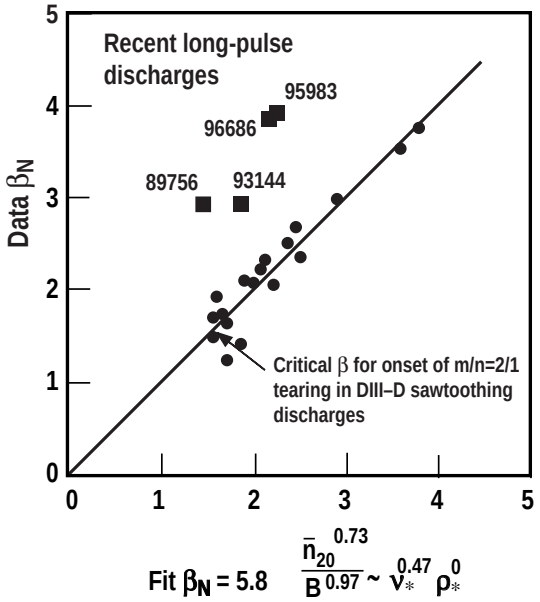

FIG. 9. The beta limit for discharges discussed in this paper (squares) exceed the NTM limit established for sawtoothing discharges (circles and line) by a factor of ~2.

many cases fishbone bursts provide the seed island, although there are also cases where the NTM trigger is not so clear. For discharge 95983 in Fig. 4, the NTM clearly starts to grow after a fishbone burst as shown in Fig. 8. Here contours of constant mode amplitude are plotted for n=1 (dark shade) and n=2 (light shade) modes. In addition to the 1/1 fishbone bursts and the associated second harmonic, one can observe the coupled 3/2 mode at ~38 kHz. The first few 3/2 bursts die away, but at 2730 ms the 3/2 mode becomes continuous and begins to grow. The 3/2 mode number has been confirmed by analyzing the poloidal magnetic probe array and by comparing the 3/2 mode frequency with the fluid rotation velocity at the q=3/2 surface. Both the seed island width and the saturation amplitude have been estimated from Mirnov signals for this discharge and agree with predictions from NTM theory.

While NTM modes appear to limit β_N in many of the high performance ELMy H–mode discharges discussed in this paper, the β_N limit is significantly higher than the limit in sawtoothing ITER-like discharges. In Fig. 9, the critical β_N for onset of NTMs is plotted versus a function of density (or collisionality ν^*) as determined by La Haye, *et al.* for sawtoothing ITER-like discharges [12]. The β_N limit for the high performance ELMing H–mode discharges discussed in this paper are also plotted and range from 50% to 100% higher than the sawtoothing limit. Despite this success in raising the NTM β limit, the NTM modes limit our ability to further increase β and, since the time at which the seed island triggers the mode varies considerably from shot to shot, the reproducibility of these discharges is poor. Techniques to calculate and produce profiles that are more robustly stable to these modes is an important next step.

4. DISCUSSION

Over the past two years, improved performance has been achieved in a variety of ELMy H–mode discharges in DIII–D. With normal-frequency ELMs (50–100 Hz), H_{98y}~1.4 (H_{89p}~2.5) and β_N~2.9 has been sustained for ~ 1.5–2 s (10–15 τ_E) in discharges with both monotonic (q_0~1) and NCS q profiles. The absence of sawteeth in these discharges plays an important role in accessing higher confinement and β relative to the ITER benchmark. In the NCS discharges, sawteeth are simply eliminated by raising q_{min} well above unity. In the monotonic q profile discharges, fishbones appear to play a role in maintaining q_0 at, or slightly above, unity, thus preventing sawteeth. Since there is no obvious reconnection of flux during fishbones, the mechanism for sustaining q_0~1 is not clear.

By removing the core sawtooth instability, more-peaked density and temperature profiles and larger core rotation (E×B shear) are observed, enabling a ~40% increase in global confinement compared with the ITER98y scaling. Although core confinement is improved in these discharges, the sharp localized ITBs seen in L–mode edge NCS discharges are not observed here.

Regarding stability, the absence of sawtooth induced seed islands allows β_N values up to 2 times the previously established neoclassical tearing mode limit. In spite of this, NTMs triggered by other MHD events (fishbones, ELMs) remain a limitation to both the reproducibility of long-pulse discharges and further attempts to increase β_N.

A new regime characterized by infrequent ELMs ($\leq$ 10 Hz) has produced performance comparable to VH–mode, but sustained for longer pulse lengths. The best of these discharges produced H_{98y}~2 (H_{89p}~3.2) and β_N~3.8 for 1 s (~5τ_E). Again, here the q profile is monotonic with q_0~1 and there are fishbones but no sawteeth. Ion thermal diffusivity is reduced over most of the discharge to ~2–3 times neoclassical. Although the ELMs are not small in this regime (2%–5% energy loss per ELM), they are benign in the sense that no global MHD mode that could cause a core β collapse is triggered. The long period between ELMs allows the stored energy and toroidal rotation time to recover, giving confinement properties that are closer to ELM-free regimes than ELMy regimes. The pulse length of most of these discharges is ultimately limited by the triggering of resistive NTMs rather than ideal MHD modes that terminate typical VH–modes.

The reasons for the improved stability are still being investigated, but we can identify several features that may be important. First, the upper single null high-triangularity shape has a high H–mode power threshold that results in a long enhanced L–mode phase. Upon the H–mode transition, high performance is obtained rapidly, before the current density in the edge region can fully develop. Although a large bootstrap peak at ρ~0.95 is observed, the average current density in the region $0.8 < \rho < 1.0$ is not so large and this is beneficial for stability to edge peeling modes. Also, the X–point is located close to the wall in these discharges which results in larger recycling near the X–point. This may have a subtle effect on details of the edge profiles and gradients.

Future plans include making use of the upcoming high-power electron cyclotron current drive (ECCD) system on DIII–D. By driving current off-axis, we will be able to achieve improved control over the q profile and can sustain the q profile for longer pulse lengths. The ECCD system will also be used for experiments on stabilizing NTMs, which are a significant limitation in long-pulse discharges.

REFERENCES

[1] LAZARUS, E.A., *et al*., Phys. Rev. Lett. **77** (1996) 2714.
[2] KOIDE, Y., *et al*., Phys. Plasma **4** (1997) 1623.
[3] SOLDNER, F.X., *et al*., Plasma Phys. Control. Fusion **39** (1997) B353.
[4] ITER Physics Basis Document, to be published in Nuclear Fusion. JET report JET-P(98)17.
[5] CHANG, Z., *et al*., Phys. Rev. Lett. **74** (1995) 4663.
[6] LA HAYE, R.J. and SAUTER, O., Nucl. Fusion **38** (1998) 987.
[7] CHAN, V.S., *et al*., in Plasma Physics and Controlled Nuclear Fusion Research 1996 (Proc. 16th Int. Conf. Montreal, 1996), Vol. 1, IAEA, Vienna (1997) 95.
[8] RICE, B.W., *et al*., to appear in Proceedings of the 25th EPS Conference on Controlled Fusion and Plasma Physics, Prague (1998)
[9] JACKSON, G.L., *et al*., Phys. Rev. Lett. **67** (1991) 3098.
[10] FERRON, J.R., *et al*., in Controlled Fusion and Plasma Physics (Proc. 21st EPS Conf. Montpellier, 1994) Vol 18B, Part I, European Physical Society, Geneva, (1994) 86.
[11] PORCELLI, F. AND ROSENBLUTH, M.N., Plasma Phys. and Contr. Fusion **40** (1994) 481.
[12] LA HAYE, R.J., *et al*., in Plasma Physics and Controlled Nuclear Fusion Research 1996 (Proc. 16th Int. Conf. Montreal, 1996), Vol. 1, IAEA, Vienna (1997) 747.